PHYSICAL REVIEW B **69**, 020103(R) (2004)

Structural complexity in binary bcc ground states: The case of bcc Mo-Ta

Volker Blum and Alex Zunger
National Renewable Energy Laboratory, Golden, Colorado 80401, USA
(Received 23 June 2003; published 23 January 2004)

Traditional sorting diagrams for ground states ($T=0$ stable atomic configurations) of bcc-based binary alloys predict simple crystal structures when simple parametric interactions (e.g., first few pairs) are assumed. However, the range and magnitude of interactions for real systems is not *a priori* known, and could lead to much greater structural complexity. We combine a density functional theory based, deterministic mixed-basis cluster expansion with an exhaustive enumeration scheme of 3×10^6 possible structures to determine the ground states of the bcc alloy Mo-Ta. The result is a rich ground-state line, changing one's outlook on bcc structural stability. We find Mo-rich (100) superlattices (including $C11_b$ and $B2$) coexisting with complex large-cell structures (Mo_4Ta_9 and Mo_4Ta_{12}). We demonstrate that a systematic cluster expansion construction scheme which includes both high-order pairs and many-body figures is a necessity to capture the ground states of Mo-Ta.

DOI: 10.1103/PhysRevB.69.020103 PACS number(s): 61.50.Ah, 61.66.Dk, 81.05.Bx, 81.30.Bx

Predicting the ground-state order (i.e., the $T=0$ stable state) of a given elemental combination has been a central challenge in metallurgy,[1,2] inorganic chemistry,[3,4] and materials theory.[5,6] Atomic ordering on a lattice is often described by coloring individual sites according to the occupying element—or, in a binary alloy, mathematically assigning spins $\sigma_i=\pm1$ to each site i. If $\boldsymbol{\sigma}$ denotes the vector of all spins σ_i, the configurational formation enthalpy $\Delta H(\boldsymbol{\sigma})$ can be exactly mapped[7] onto the pair and multisite *interatomic interactions* J of an Ising-like Hamiltonian

$$\Delta H(\boldsymbol{\sigma})=J_0+\sum_i \sigma_i J_i+\sum_{i,j} J_{i,j}\sigma_i\sigma_j+\sum_{i,j,k} J_{i,j,k}\sigma_i\sigma_j\sigma_k + \cdots, \quad (1)$$

the defining equation of a cluster expansion (CE).[8] This representation has been used extensively in attempts to provide maps of ground-state ordering, treating the set $\{J\}$ as formal parameters (see for instance Refs. 9–13): For restricted sets of interactions, truncated by intuition to, e.g., first- and second-nearest neighbors, one can enumerate all possible ground states of Eq. (1) and classify them according to the interaction values which produce them. For example, assuming just a nearest neighbor J, only the $B2$ (CsCl-type) structure can be stabilized in bcc. If one adds a second-nearest-neighbor interaction, the $B32$ (LiAl-type) and $D0_3$ (BiF_3-type) structures become additionally possible. Finally, when three pair interactions are allowed, at least 17 distinct structures with up to 12 atoms per unit cell are possible ground states.[12–13] At first glance, third-nearest pair interactions for bcc would seem sufficient in the sense that the five simple, commonly observed ground states[13] $B2$, $B32$, $D0_3$, $C11_b$, and $B11$ are then all allowed ground-state structures. Many studies of actual bcc alloys truncate to this interaction set,[14–18] so more complex bcc-based ground states are not explained even for the case (Li-Al) where such structures are known experimentally.[19] One needs to determine whether simple interactions are really characteristic of bcc-based alloys and their ground states, or whether the physical interactions of actual bcc systems will lead to structurally complex ground states which are overlooked by few-interaction ground-state maps.

In the present work, we tackle the ground-state problem from the inverse point of view. Based on the mixed-basis cluster expansion (MBCE) method,[20,21] we apply an iterative, deterministic scheme to calculate the interactions $\{J\}$ of Eq. (1) for Mo-Ta. These interactions are obtained via an electronic-structure theory (the density-functional method) which includes, in principle, various types of bonding forces. We then predict the ground-state structures from Eq. (1). The key result is *the emergence of bcc-based ground state structures of a complexity which is not foreseen by truncated pair-only Hamiltonians.* We find that only a delicate balance of long-ranged pair and multisite interactions can reflect the coexistence of these ground-state structures.

The goal of the MBCE method is to provide Ising-like interactions [Eq. (1)] which describe the configurational energetics of arbitrarily complex binary alloys with the accuracy achieved by modern electronic-structure theory for simple ordered structures. Here, the deterministic procedure itself (not the user) decides the number and type of interactions that are needed to describe a particular material system. The MBCE method has been reviewed elsewhere,[8,21] and will only be briefly summarized here. Equation (1) is rewritten to expand $\Delta\tilde{H}=\Delta H-E_{\rm ref}$ in terms of symmetry-equivalent pair and many-body figures f, so that

$$\Delta\tilde{H}_{\rm CE}(\boldsymbol{\sigma})=J_0+(2x-1)J_1+\sum_p^{n_p} J_p D_p \overline{\Pi}_p(\boldsymbol{\sigma}) + \sum_{\rm MB's} J_{\rm MB} D_{\rm MB} \overline{\Pi}_{\rm MB}(\boldsymbol{\sigma}), \quad (2)$$

with interaction parameters J_f and symmetry-degeneracy D_f for each inequivalent f. The configuration dependence is contained only in the lattice-averaged correlation functions $\overline{\Pi}_f(\boldsymbol{\sigma})$. The "constituent strain" energy $E_{\rm CS}(\boldsymbol{\sigma})$ is chosen[20] for $E_{\rm ref}$. The interactions $\{J_f\}$ are obtained by mapping $\Delta\tilde{H}_{\rm CE}(\boldsymbol{\sigma})$ to an appropriate input base of fully relaxed $\{\Delta\tilde{H}_{\rm LDA}(\boldsymbol{\sigma})\}$, calculated by density functional theory in the local-density approximation (DFT-LDA) for a set of N_σ structures. The key task of the MBCE is to identify the *relevant* figures f and their interaction energies J_f for a specific

alloy system. In the present work, we apply a three-level, iterative construction scheme:

(i) For a given number n_p of pairs and a set of nonpair interactions $\{J_{\mathrm{MB}}\}$, one first obtains an optimum interaction set $\{J_f\}$ by minimizing[8,20]

$$s_{\mathrm{MBCE}}=\sum_{\sigma} w_\sigma|\Delta\tilde{H}_{\mathrm{LDA}}(\boldsymbol{\sigma})-\Delta\tilde{H}_{\mathrm{CE}}(\boldsymbol{\sigma})|^2+\frac{t}{\alpha}\sum_{p}^{n_p} R_p^{\lambda}D_pJ_p^2. \tag{3}$$

Here, the usual least-squares sum is amended by an additional constraint per pair. This allows for an unlimited number of pair interactions, and avoids an unphysical cutoff dictated by the finite number of input structures. The proper spatial decay of J_p with pair distance R_p is enforced by weight factors R_p^{λ}, with t a Lagrangian multiplier and $\alpha=(\Sigma_p^{n_p}\sqrt{R_p^{\lambda}/D_p})^2$ a normalization factor.

(ii) Different sets $\{n_p,t,\lambda\}$ and $\{J_{\mathrm{MB}}\}$ are compared using a cross-validation[22] (CV) criterion to ensure a *predictive* MBCE for energies of structures not included in the fit of Eq. (3). Earlier applications of the MBCE (Refs. 8,21) successfully used "hold-out-set" CV: Of a total number N_σ of structures for which ΔH_{LDA} are available, only $N_\sigma-N_v$ are used for the fit of Eq. (3), and the rest used for predictions. Recently, van de Walle and Ceder[23] successfully applied "leave-one-out" CV for this task. In the spirit of Shao's work,[24] our implementation of choice in the present work is "*leave-many-out* CV": From a total of N_σ structures, pick N_p subsets ("exclusion sets") of N_v structures each. For each exclusion set i, use only the remaining $N_\sigma-N_v$ structures to fit Eq. (2) by minimizing s_{MBCE} [Eq. (3)]. The N_v structures excluded from the fit of Eq. (2) are reserved for prediction testing: After fitting the interactions of Eq. (2), we calculate $\Delta H_{\mathrm{CE}}^{(i)}(\boldsymbol{\sigma})$ for the N_v excluded structures and compare to their known ΔH_{LDA}. The average prediction error over all exclusion sets is

$$s_{\mathrm{cv}}=\frac{1}{N_pN_v}\sum_{i}^{N_p}\sum_{\sigma\epsilon\ \mathrm{set}\ i}|H_{\mathrm{CE}}^{(i)}(\boldsymbol{\sigma})-H_{\mathrm{LDA}}(\boldsymbol{\sigma})|^2. \tag{4}$$

We choose N_p and N_v such that every input structure appears at least twice in the exclusion sets (e.g., $N_p=12$, $N_v=12$ for the final 56 ΔH_{LDA}).

(iii) We iteratively increase the size N_σ of the LDA input set $\{\Delta H_{\mathrm{LDA}}(\boldsymbol{\sigma})\}$. In each iteration (fixed LDA input set), we minimize s_{cv} to identify promising combinations $\{n_p,t,\lambda\}$ and $\{J_{\mathrm{MB}}\}$ ("candidate CE's"). We then predict the ground states of the candidate CE's and calculate ΔH_{LDA} for some of these to verify the CE's true predictive power. The newly calculated ΔH_{LDA} are then added to the N_σ input structures. The procedure is repeated until the prediction errors become sufficiently low and the predicted ground-state line agrees with LDA.

In the present work, $\Delta\tilde{H}_{\mathrm{LDA}}(\boldsymbol{\sigma})$ were obtained in the local-density approximation to density-functional theory, using the momentum-space total-energy method as implemented in the VASP program package.[25] Mo and Ta were represented by projector-augmented wave potentials including $4p$ and $5p$ semicore states, respectively, together with the exchange-correlation functional of Perdew and Zunger.[26]

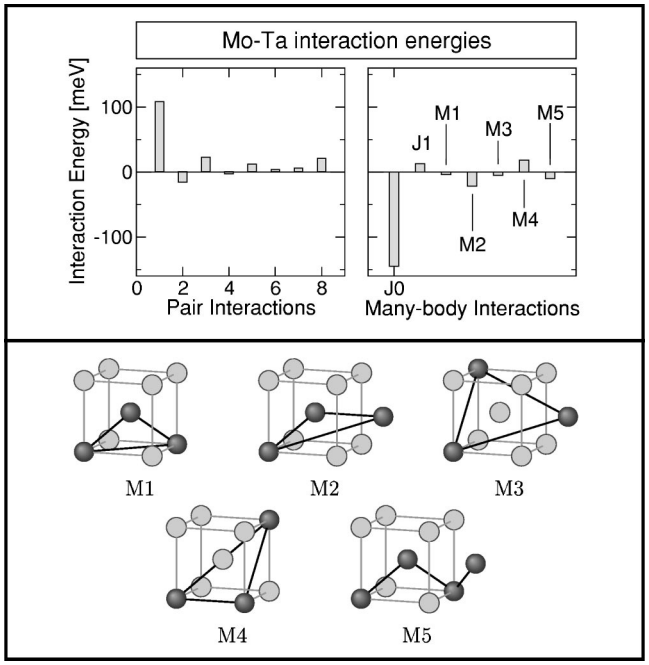

FIG. 1. Upper panel: Symmetry-weighted pair and many-body interactions D_fJ_f obtained in the cluster expansion of Mo-Ta, fitted with MBCE constraints $t=9$ and $\lambda=4$. Lower panel: definition of the figures.

We conducted k-space basis convergence tests which ensure convergence of ΔH_{LDA} at the meV level. These tests show $E_{\mathrm{cut}}=250$ eV to be sufficient. Wherever ΔH_{LDA} can be calculated using equivalent k points,[27] $12\times12\times12$ grids (pertaining to the cubic bcc unit cell) or denser are employed. In the few cases where this method proves impractical, k-grid convergence was achieved explicitly.

The MBCE for Mo-Ta was constructed in five iterations of increasing LDA data base size, beginning with a 24-structure set of small-cell configurations, including the usual suspects $B2$, $B32$, $B11$, $C11_b$, and $D0_3$, up a total of $N_\sigma=56$ input $\Delta H_{\mathrm{LDA}}(\boldsymbol{\sigma})$ values. The final CE features five many-body figures and eight pair interactions, shown in Fig. 1. Notably, it includes both high-order pairs and many-body terms of considerable magnitude. These interactions yield a fit error of 2.5 meV for all 56 input configurations, with a maximum deviation of only 6.3 meV. The predictive accuracy of the CE is $s_{\mathrm{cv}}=3.6$ meV, i.e., less than 2% of $\Delta H_f(B2,\mathrm{MoTa})$.

With the converged MBCE, we can investigate the physical ground-state line of Mo-Ta. We use the enumeration scheme of Ref. 28 to predict ΔH_{CE} of all 3×10^6 possible configurations with up to 20 atoms per unit cell. For negative ΔH, ground states can be read from a plot of $\Delta H_{\mathrm{CE}}(\boldsymbol{\sigma})$ versus composition as the breaking points of the convex hull about all structures. This ground-state line is shown in Fig. 2. The structures associated with several breaking points are shown in Fig. 3, and collected in Table I, together with the "depth" Δ of each breaking point with respect to the phase-separated limit (concentration-weighted average) of the adjacent breaking points. Also listed are transition temperatures T_c for each ground state obtained from canonical Monte

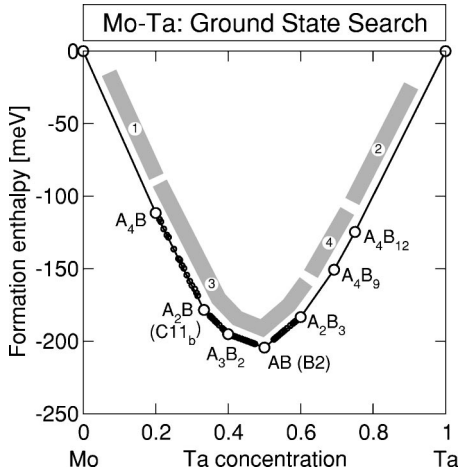

FIG. 2. Ground-state line from exhaustive search of structures up to 20 atoms per unit cell (3×10^6 structures). Four qualitatively different regions are highlighted (A=Mo, B=Ta).

Carlo simulations (cell sizes $20\times20\times20$ or larger, 2000 or 4000 flips per site) based on the converged MBCE.

Ground states with sufficiently large Δ are identified as large circles in Fig. 2. Here, the Mo-Ta system is divided into four structurally distinct regions. (i) In *region 1*, the Mo-rich range below 20% Ta, we find several possible, very shallow ground states. However, with $\Delta\lesssim2$ meV, they are very close to the phase-separated limit of pure Mo and Mo_4Ta, so that we did not investigate this range in greater detail. (ii) In *region 2*, on the Ta-rich side (above 75% Ta), no ground states are found. The interesting regions are 3 and 4: (iii) In *region 3* (roughly 20–60% Ta) we find five distinct small-cell ground states, denoted A_4B, A_2B, A_3B_2, AB, and A_2B_3

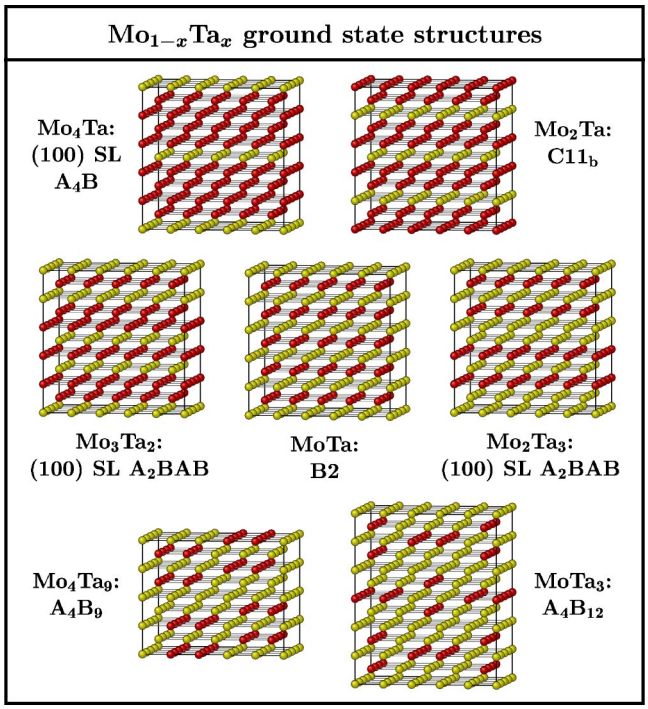

FIG. 3. Ground-state structures in regions 3 (20–60 % Ta) and 4 (60%–80% Ta) of the Mo-Ta ground-state line.

TABLE I. Ground-state structures in Mo-Ta, their energetic depths, and Monte-Carlo calculated critical temperatures. MBCE values for Δ are given and compared to LDA (brackets).

Composition	Structure	Δ [meV]	T_c [K]
Mo_4Ta	(100) SL A_4B	<4.5 (<4.0)	195
Mo_2Ta	$C11_b$	11.2 (11.7)	400
Mo_3Ta_2	(100) SL A_2BAB	6.3 (6.2)	275
MoTa	$B2$	15.1 (17.0)	600–1000[a]
Mo_2Ta_3	(100) SL A_2BAB	6.9 (2.0)	610
Mo_4Ta_9	(Figure 3)	3.5 (6.9)	490
Mo_4Ta_{12}	(Figure 3)	2.2 (1.0)	385

[a]Second-order transition.

in Fig. 2 (A=Mo, B=Ta). These structures are depicted in Fig. 3. Each is a superlattice (SL) of pure (100) planes: the well-known $B2$ and $C11_b$ structures [AB and A_2B (100) SL's, respectively], the larger A_4B (100) SL and the hybrid A_2BAB (100) SL's of composition Mo_3Ta_2 and Mo_2Ta_3. In addition, the MBCE predicts an exceedingly low enthalpy for the inclusion of antiphase defects between the basic (100) superlattice units. Therefore, region 3 contains a quasicontinuum of more complex (100) SL's, which are energetically extremely close to the ground-state line [black dots in Fig. 2(b)]. These higher-order SL's are ''building-block'' combinations of the five basic breaking points: Sequences $(A_4B)_m(A_2B)_n$ populate the ground-state line between 20% and 33% Ta, changing to $(A_2B)_m(A_2BAB)_n$ between 33% and 40% Ta, $(A_2BAB)_m(AB)_n$ between 40% and 50% Ta, and $(AB)_m(AB_2AB)_n$ between 50% and 60% Ta. (iv) *Region 4* shows only two breaking points. The underlying ground-state structures A_4B_9 and A_4B_{12}, also shown in Fig. 3, have 13 and 16 atoms per unit cell. They are structurally quite distinct from the Mo-rich (100) superlattices. In fact, no simple superlattice notation can represent both A_4B_9 and A_4B_{12} consistently. They are based on (100)-oriented columns of Mo-atoms embedded into a Ta matrix, and placed at regular 2nd and 4th nearest-neighbor distance from one another. In further contrast to region 3, both are isolated structures rather than part of a quasicontinuous series. Although remarkably deep in LDA (Table I), it would be impossible to guess both structures within an intuition-based approach of ''rounding up the usual suspects.'' A_4B_9 and A_4B_{12} are true predictions of the MBCE construction process, and testaments to the power of a systematic, material-specific ground-state search.

The Mo-Ta phase diagram[29] shows only a high-temperature solid solution, and the absence of long-range order in Mo-Ta has been verified experimentally for samples sintered at 1773 K and 673 K.[30] This is consistent with our predicted low T_c's (Table I). However, there are experimental indications that order does exist. The measured enthalpy of mixing is negative:[31] e.g., $\Delta H_{\mathrm{mix}}(x=0.5)=-114\pm26$ meV. In comparison, our MBCE predicts -127 meV for the fully random state. Also, short-range order induced x-ray diffuse intensity maxima occur at the (100) position in

reciprocal space for 79% Mo and 63% Mo solid solutions.[32] This is confirmed by simulations based on our converged MBCE.

The ground-state structures of regions 3 and 4 are unsuspected in that they cannot exist within a few-interaction ground-state enumeration scheme:[12,13]

Necessity of high-order pairs: The (100) SL ground states of region 3 are equivalent to one-dimensional Ising lattices with suitably renormalized interplanar instead of interatomic interactions. To be stable, A_4B and A_2BAB superlattice-type ground states require[12] at least fourth nearest interplanar interactions—in terms of the bcc interatomic interactions this means we must use 6th and 8th neighbors. Any shorter-ranged CE or ground-state map must inevitably miss A_4B and A_2BAB as stable ground states.

Necessity of many-body interactions: The complex ground states of region 4 and those of region 3 are situated in complementary concentration ranges, i.e., the energetic hierarchy of structures changes when switching from composition $A_{1-x}B_x$ to A_xB_{1-x}. In our MBCE, this can only be described by odd-body (here three-body) figures, which are therefore indispensable to capture the ground-state line of Mo-Ta.

We illustrate the effect of high-order interactions by systematically peeling off some of them from the converged MBCE of Fig. 1, and repeating the ground-state search. In each case, the remaining J are refit to the LDA input database. (i) Removing all the many-body terms from the MBCE places the $C11_b$ structure on the Ta-rich ground-state line at $MoTa_2$, although it is not a ground state of the converged MBCE. The actual ground-state structures A_4B_9 and A_4B_{12} are eliminated. Instead, A_4B_{12} now appears as a false ground state on the Mo-rich side, displacing the true ground state, the A_4B (100) SL, and the quasicontinuum of SL's up to $C11_b$. (ii) Further restricting the CE to *only five pairs* removes also the (100) SL's A_2BAB from the ground-state line. Except for some shallow, spurious states in region 1, the ground-state line now shows only $C11_b$ (Mo_2Ta), $B2$ (MoTa), and $C11_b$ ($MoTa_2$). (iii) *A minimal cluster expansion:* A common approach to CE is the Connolly-Williams (CW) method,[33] where only the shortest-ranged terms are fitted to an equal number of guessed input structures. We demonstrate the effect on ground states by examining a bcc CW approach.[15–17] Here, six input structures, bcc (Mo and Ta), $D0_3$ (Mo_3Ta and $MoTa_3$), $B2$ (MoTa), and $B32$ (MoTa), are used to fit the six shortest bcc interactions, spanning a maximum distance of second-nearest neighbors. This CE shows only two ground states, $D0_3$ (Mo_3Ta) and $B2$ (MoTa). Moreover, the predicted $T_c = 1800$ K for the $A2$-$B2$ transition is now excessively high compared to $T_c < 1000$ K of the converged CE (Table I).

In summary, Mo-Ta reveals an unexpected and feature-rich ground-state line. Instead of a few ''usual-suspect'' structures only, there are at least seven distinct ground states, in part of a complexity reaching beyond mere intuition. Their prediction would be impossible with approaches restricted to such intuition: short-ranged CE's in the style of CW[33] discussed above, or ground-state enumeration schemes based on few interactions only.[9–13] This work was supported by DOE-SC-BES-DMS under Grant No. DEAC36-98GO10337.

[1] W. Hume-Rothery and G. Raynor, *The Structure of Metals and Alloys* (Institute of Metals, London, 1954).
[2] J. Friedel, *The Physics of Metals* (Cambridge University Press, London, 1969).
[3] L. Pauling, *The Nature of the Chemical Bond* (Cornell University, Ithaca, 1960).
[4] A. Wells, *Structural Inorganic Chemistry* (Clarendon, Oxford, 1975).
[5] A. Khatchaturyan, Prog. Mater. Sci. **22**, 1 (1978).
[6] A. Zunger, Phys. Rev. B **22**, 5839 (1980).
[7] J. Sanchez, F. Ducastelle, and D. Gratias, Physica A **128**, 334 (1984).
[8] A. Zunger, in *Statics and Dynamics of Alloy Phase Transformations*, edited by P. Turchi and A. Gonis (Plenum, New York, 1994), pp. 361–419.
[9] J. Kanamori, Prog. Theor. Phys. **35**, 16 (1966).
[10] S. Allen and J. Cahn, Acta Metall. **20**, 423 (1972).
[11] J. Kanamori and Y. Kakehashi, J. Phys. (Paris) **38**, 274 (1977).
[12] A. Finel, Ph.D. thesis, Université de Pierre et Marie Curie, 1987.
[13] F. Ducastelle, *Order and Phase Stability in Alloys* (North-Holland, Amsterdam, 1991).
[14] M. Sluiter, D. de Fontaine, X.Q. Guo, R. Podloucky, and A.J. Freeman, Phys. Rev. B **42**, 10 460 (1990).
[15] A. Pasturel, C. Colinet, A. Paxton, and M. van Schilfgaarde, J. Phys.: Condens. Matter **4**, 945 (1992).
[16] G. Rubin and A. Finel, J. Phys.: Condens. Matter **7**, 3139 (1992).
[17] G. Das, A. Arya, and S. Banerjee, Intermetallics **4**, 625 (1996).
[18] P. Turchi, A. Gonis, V. Drchal, and J. Kurdnovsky, Phys. Rev. B **64**, 085112 (2001).
[19] M. Sluiter, Y. Watanabe, D. de Fontaine, and Y. Kawazoe, Phys. Rev. B **53**, 6137 (1996).
[20] D. Laks, L. Ferreira, S. Froyen, and A. Zunger, Phys. Rev. B **46**, 12 587 (1992).
[21] A. Zunger, L. Wang, G. Hart, and M. Sanati, Modell. Simul. Mater. Sci. Eng. **10**, 1 (2002).
[22] See M. Plutowski, *Survey: Cross-validation in theory and practice*, http://www.emotivate.com/CvSurvey.doc (1996).
[23] A. van de Walle and G. Ceder, J. Phase Equilib. **23**, 348 (2002).
[24] J. Shao, J. Am. Stat. Assoc. **88**, 486 (1993).
[25] G. Kresse and J. Furthmüller, Comput. Mater. Sci. **6**, 15 (1996).
[26] J. Perdew and A. Zunger, Phys. Rev. B **23**, 5048 (1981).
[27] S. Froyen, Phys. Rev. B **39**, 3168 (1999).
[28] L. Ferreira, S.-H. Wei, and A. Zunger, Int. J. Supercomput. Appl. **5**, 34 (1991).
[29] *Phase Equilibria, Crystallographic and Thermodynamic Data of Binary Alloys*, edited by B. Predel, Landolt-Börnstein, New Series, Group IV, Vol. 5H (Springer, Berlin, 1997).
[30] G. Geach and D. Summers-Smith, J. Inst. Met. **80**, 143 (1951–52).
[31] S. Singhal and W. Worrell, in *Metallurgical Chemistry*, edited by O. Kubaschewski (Her Majesty's Stationary Office, London, 1974), pp. 65–72.
[32] B. Predmore and R. Arsenault, Scr. Metall. **4**, 213 (1970).
[33] J. Connolly and A. Williams, Phys. Rev. B **27**, 5169 (1983).